

Using MRI to characterize lymphatic structure and function without exogenous contrast agents

Paula Donahue¹, Swati Rane², Seth Smith², and Manus Donahue²

¹Physical Medicine and Rehabilitation, Dayani Center for Health and Wellness, Vanderbilt University School of Medicine, Nashville, TN, United States, ²Radiology, Vanderbilt University School of Medicine, TN, United States

Target Audience: Researchers interested in noninvasive lymphatic imaging and emerging clinical applications of chemical exchange saturation transfer (CEST) MRI.

Purpose: The overall objective is to translate noninvasive MRI techniques for measuring brain structure and function to the lymphatic system to characterize axillary (i) lymphatic node volume, (ii) lymphatic vessel diameter, (iii) lymph flow velocity, and (iv) interstitial protein accumulation in patients with breast cancer-related lymphedema (BCRL). Lymphedema is a chronic condition impacting 3-5 million Americans, with reported incidence as high as 94% in breast cancer survivors undergoing lymph node resection¹. With reduced lymphatic flow velocity, protein accumulates in the interstitial space leading to limb swelling which then requires lifelong management. Clinically, evaluation of lymphedema interventions relies on patient-reporting and circumferential limb volume measurements. MRI techniques used to characterize lymphatic dysfunction are extremely limited and may involve exogenous agents which are suboptimal in cases of lymphedema as they alter the physiological environment and stress an already compromised system. Recently reported 3T lymphatic T1 and T2 measurements have been used to guide development of protocols for measuring human lymphatic flow velocity non-invasively *in vivo*². Here, protocols for non-invasive structural imaging of lymphatic vessels, and characterization of interstitial protein accumulation using amide proton transfer (APT) CEST MRI³, are evaluated in healthy and compromised lymphatic systems by exploiting parallel RF transmit in conjunction with multi-channel torso receive coils. The hypothesis to be investigated is that following appropriate protocol adjustments including customized fat suppression, localized shimming, and contrast adjustment (i.e., through appropriate choice of TR/TE/TI), MRI protocols with established relevance in the brain can be translated to visualize disruptions in lymphatic system function and structure in patients with mild and moderate lymphedema.

Methods: A multi-faceted, noninvasive 3T MRI protocol for characterizing lymphatic system structure and function was optimized *ex vivo* and subsequently implemented *in vivo* in healthy volunteers (n=10) and patients (n=4) with unilateral BCRL. Structurally, this included high spatial resolution visualization of (i) axillary lymph nodes (diffusion-weighted-imaging-with-background-suppression, DWIBS) and (ii) vessels (3D turbo-spin-echo); and functionally, characterization of (iii) lymphatic flow velocity (spin labeling), and (iv) protein accumulation in the interstitial tissue (APT CEST). In all methods except CEST, a spectral presaturation with inversion recovery prepulse frequency-selective for fat was used (7.5 ms; bandwidth = 190 Hz) for optimized fat suppression immediately before the RF excitation. Scan parameters: 3D TSE: turbo factor = 124; spatial resolution = 1 x 1 x 10 mm; TE/TR=600/5000 ms; slices = 30, SENSE-factor = 2.5, averages = 4. DWIBS: spatial resolution=3x3x5 mm; b-value=800 s/mm²; TR/TE/TI=8037/49.8/260 ms. Spin Labeling: TE=4 ms; spatial resolution, 3x3x5 mm; SENSE-factor=2; half scan factor=0.6; signal averages=9; TI=500-10,000 ms, and single-shot gradient-echo EPI. CEST: slices=16, B₁=100 ms 1 μ T sinc-gauss pulse, spatial resolution=0.8x0.8x5 mm³, $\Delta\omega$ = +6 - -6 ppm at 0.25 ppm spacing; 3D segmented gradient echo. A Mann-Whitney U-test was used to test significance between patients/controls and affected/unaffected limbs. Owing to different stages of development, not all methods were applied in all subjects.

Results and Discussion: A reduction ($P<0.01$) in lymphatic flow velocity in the affected arms of patients with unilateral BCRL was observed and the ratio of unaffected to affected axilla lymphatic velocity (1.24 \pm 0.18) in moderately impaired (Stage II) BCRL patients was significantly ($P<0.01$) higher than the left to right ratio found in healthy subjects (0.91 \pm 0.18). Symmetric CEST contrast (Fig. 1) was observed in healthy limbs (right/left ratio: 0.01 \pm 0.05), but significantly ($P<0.01$) increased CEST contrast was observed on the affected side of the Stage 0 (i.e., pre-clinical) lymphedema patient (affected/unaffected: 0.05 \pm 0.08), consistent with asymmetric protein accumulation in the interstitial space. In this patient, the CEST contrast was observed in the absence of any overt changes in lymph volume as visualized on

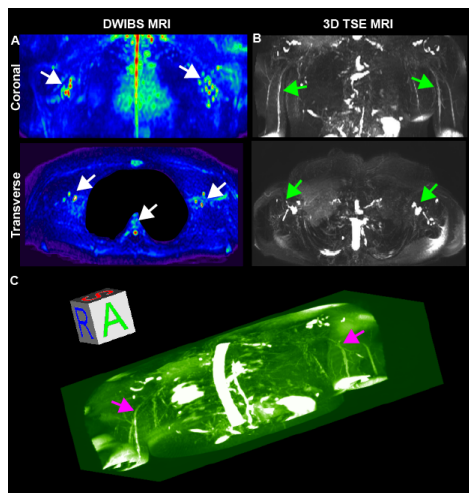


Fig. 2. Noninvasive visualization of lymphatic structure at 3.0T. (A) DWIBS sequence allows for visualization of axillary lymph nodes (white arrows; coronal and transverse slices shown). (B) The long TE 3D TSE approach allows for visualization of lymph vessels (green arrows). Note: At this long TE, it is not possible for this contrast to be due to blood water, as blood water T_2 is only 10-150 ms (depending on oxygenation and hematocrit). (C) 3D maximum intensity projection reconstruction allows for 3D reconstruction and volumetric assessment of lymph in vessels (purple arrows).

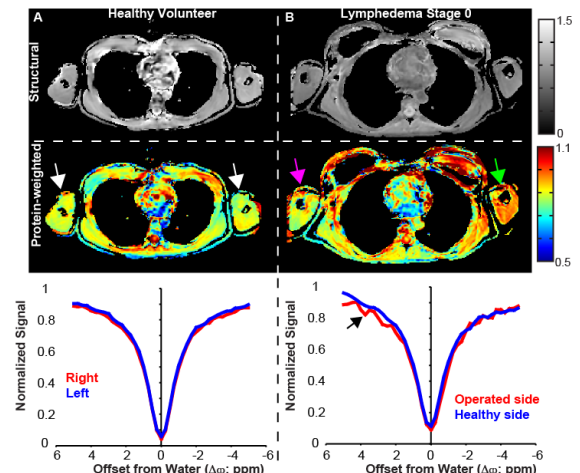


Fig. 1. T1-weighted structural and APT maps for a healthy volunteer (A) and Stage 0 unilateral BCRL patient (B). Structural imaging is unremarkable. APT maps of the +3.5 ppm effect in right/left arms of healthy volunteers (white arrows) are largely symmetric, however the patient demonstrates reduced signal on the lymphedema side (pink arrow and red z-spectrum) compared with unaffected side (green arrow), consistent with increased protein accumulation. APT CEST shows contrast not apparent from structural imaging alone.

the high-resolution structural image of the lymph vessels (Fig. 2), suggesting that measurements of protein accumulation in tissue may be a more sensitive indicator of impairment, and in turn rehabilitation response, in early disease stages. We demonstrate the utility of noninvasive MRI to quantitatively assess multiple lymphatic properties, thus providing a foundation for clinical investigations where lymphedema etiology and therapeutic interventions may be interrogated without exogenous agents on persons with lymphedema. Clinical research using this MRI protocol can further investigate best care

Conclusion: We demonstrated the utility of noninvasive MRI to quantitatively assess multiple structural and functional characteristics of healthy and diseased lymphatic systems. Results are intended to motivate larger-scale studies that expand applications of functional and chemical MRI to the lymphatic system.

References: 1. DiSipio T, et al. *Lancet Oncology*. 2013;14:500-15. 2. Rane S et al. *Radiology*. 2013 July 17. 3. Zhou J, et al. *Nat Med*. 2003;9: 1085-90.